Proceedings of ASME Turbo Expo 2011
GT2011
June 6-10, 2011, Vancouver, British Columbia, Canada

GT2011-45607

SINGLE AND MULTI OBJECTIVE CFD OPTIMIZATION OF HORIZONTAL AXIS WIND TURBINES

Fabio De Bellis
Polytechnic University of Bari
Dept. of Mechanical and Management Engineering
Via G. Re David, 70125, Bari, Italy

Luciano A. Catalano
Polytechnic University of Bari
Dept. of Mechanical and Management Engineering
Via G. Re David, 70125, Bari, Italy

ABSTRACT

In spite of the enlarging interest in wind turbines development, the design optimization of wind turbine blades has not been studied in the past as gas or steam turbines optimization. Due to its reduced computational cost, Blade Element Momentum (BEM) method has been employed up to now to estimate the power output of the turbine. However, BEM method is not able to predict complex three dimensional flow fields or the performance of profiles for which drag and lift coefficients are not available.

Theoretically, Computational Fluid Dynamics (CFD) can be more useful in these cases, but at the price of a much higher overall computational cost.

In a past work, the authors developed and validated a simplified CFD process (including meshing) capable to assess the aerodynamic loads acting on a wind turbine with acceptable computational resources. Starting from that, in this work a full 3D CFD optimization of a small wind turbine is presented, both with constrained single- and multi- objective. Twist and chord distributions of a single blade have been varied keeping fixed the aerodynamic profile, and the obtained optimums have been compared with a benchmark case.

The results demonstrate that CFD optimization can be effectively employed in a wind turbine optimization. As expected, stalled conditions of the blade are more likely to be improved than those characterized by attached flow. Future works will focus on multi-disciplinary optimization and will include also aerodynamic profile variation.

INTRODUCTION

In the last ten years, wind turbines demand had grown steeply, giving a 15.5% increment of installed power in Europe only in 2009 [1], which becomes 31% worldwide [2]. Competition between different manufacturers increased as well, and nowadays there is a great interest regarding the possible improvements of existing designs and the development of innovative concepts. Nevertheless, the design optimization of wind turbines is not as common as gas or steam turbines optimization, which is a widespread and well documented practice [3-6]. Usually wind turbine researchers focused their attention on the optimization of the installation site matching or on the control systems [7,8], but there are very few works available in the literature about the optimization of the turbine design by itself [9-12]. However, such papers employed Blade Element Momentum (BEM) method to evaluate the performance of the turbine. A complete description of the BEM method can be found in [13], but it is worthwhile to recall two key aspects of it. Firstly, in BEM method the blade is divided in many sections in the spanwise direction and each of them is independent from the others: this is the hypothesis of ‘no radial dependency’. Due to its hypothesis, radial flows cannot be considered in BEM computations and the flow in each section is locally treated as 2D. Secondly, all the calculations of the loads acting on a single section are based on normal and tangential force coefficients, which in turn depend on the lift and drag measured coefficients of the local profile, accordingly to the following equations:

$$C_N = C_l \cos\Phi + C_d \sin\Phi \tag{1}$$

$$C_T = C_l \sin\Phi - C_d \cos\Phi \tag{2}$$

where Φ is the angle between the plane of rotation and the relative velocity. Such assumptions lead to the following implications.

1. Three dimensional effects and secondary flows in the spanwise direction are not taken into account in a BEM computation, whereas for example stall is a three dimensional phenomenon.
2. BEM method cannot be employed when lift and drag coefficients of the section profile are not known *a priori* from experimental campaigns; that is, a BEM optimization is limited to existing and measured aerodynamic profiles.
3. Lift and drag coefficients of the profiles are measured in non-rotating conditions; then, the BEM method computes the performance of a rotating blade without considering the non-inertial effects introduced by the rotation.

Nevertheless, it should be pointed out that some corrections (especially Prandtl and Glauert) were introduced to mitigate the effects of the aforementioned implications, and BEM method was extensively applied in the past to wind turbine design and optimization, particularly due to its low computational cost.

In order to consider the effects of three dimensional and rotational flows however, Computational Fluid Dynamics (CFD) may be theoretically regarded as the best option, because no assumptions are made in advance about the flow behavior. In a CFD algorithm in fact Navier-Stokes equations are solved locally on each grid cell composing the domain; however, numerical approximations can be significant and computational resources are a serious issue. In addition, CFD is the only option available when the lift and drag coefficients of the aerodynamic profile are not know (innovative or modified profiles).

It was demonstrated in the past that CFD can be successfully employed to assess the aerodynamics of wind turbines [14-18]. Unfortunately, the complexity of the flow field, which is unsteady, rotational, full three dimensional and with high Reynolds numbers, requires severe resources to be simulated with acceptable accuracy by CFD. As a consequence, CFD optimization of wind turbines had not been considered affordable up to now, and no works are available in the literature on this topic. Considering that a “classic” optimization can require tens or even hundreds of evaluations (depending on the numbers of objectives), if a wind turbine CFD optimization has to be performed there are two possibilities: the availability of a huge amount of computational resources (including time) or the development of a CFD simulation technique at the same time affordable and reliable. The latter option was investigated by the authors in a past work [19], where the feasibility of such approach was demonstrated. In that paper the whole CFD process was analyzed and, starting from mesh generation, some simplifications were introduced, such as fully unstructured mesh topology, reduced grid size, incompressible flow assumption, use of wall functions, commercial available CFD package employment. The chosen final settings were the result of a trade-off between numerical accuracy and resources utilized: in this way, the aerodynamic performance of a wind turbine blade was assessed with significantly less computational power. Besides the introduced simplifications, numerical predictions of shaft torque, forces and flow distribution showed a confident agreement with the NREL Phase VI experimental data set [20].

Such achievements allow now to develop the CFD optimization of a stall regulated wind turbine, which is the matter studied in the present work. The aim of this work is to assess the feasibility of a full 3D CFD optimization of horizontal axis wind turbine (HAWT), and the results presented before the conclusions show that the technique can be successfully employed for this purpose, even without modifying the aerodynamic profile. The proposed method has been applied to a small wind turbine (10 m diameter) in order to be compared with a well known benchmark of the same diameter, but in principle it could be applied to any other HAWT size. In the next section the methodology employed to design a HAWT is discussed, from geometry parameterization to optimization algorithms.

METHODOLOGY

Geometry Parameterization

The very first step in an optimization process is the geometry parameterization: the main target is to reduce as much as possible the number of parameters necessary to completely describe a very elaborate three dimensional body like a wind turbine blade. In fact, the computational effort of the optimization algorithm increases with the number of variables, due to the enlarged complexity of the objective functions.

For simplicity reasons then, in the present study the airfoil profile has been kept fixed along the blade span and equal to the one employed in the benchmark case, the aforementioned NREL Phase VI turbine [20], that is the S809 profile originally designed by Tangler et al. [21].

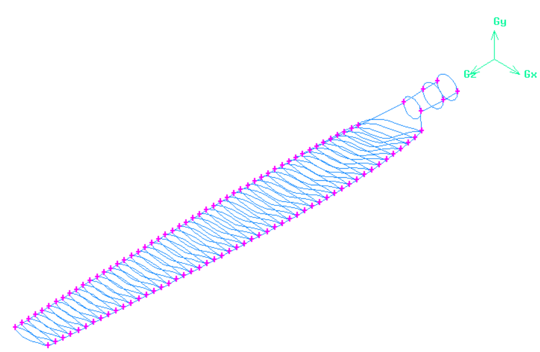

Fig. 1 – The blade is constructed from 50 stacked sections, each of them defined by its twist and chord values.

The blade is divided in 50 sections in the radial direction, and for each span section only the values of local chord and twist are varied. Since the profile is fixed, each section is completely defined by its twist and chord, and the complete blade is constructed stacking one upon the other the successive sections (a root segment with transition from the S809 to a circular profile is added, whilst the twist axis is fixed at 30% of the chord), as shown in Fig. 1.

As a consequence, the construction of a blade should require 100 parameters, but in order to reduce the number of variables involved and to obtain smooth distributions, it has been preferred to parameterize the twist and chord distributions instead. Twist distribution has been defined by a third order polynomial, whereas the chord distribution by a first order polynomial, as in the equations below:

$$a_1 \left(\frac{r_i}{R}\right)^3 + a_2 \left(\frac{r_i}{R}\right)^2 + a_3 \left(\frac{r_i}{R}\right) + a_4 = t_i \, [°] \tag{3}$$

$$b_1 \left(\frac{r_i}{R}\right) + b_2 = c_i \, [m] \tag{4}$$

where r_i is the span station value, R is the blade span (equal to 5 m) and **A** and **B** are the vectors of coefficients of the two curves, the former composed by 4 elements and the latter by 2, resulting in a total of 6 design variables. In such a way, a twisted and tapered blade can be produced starting from just 6 parameters, as represented in Fig. 2.

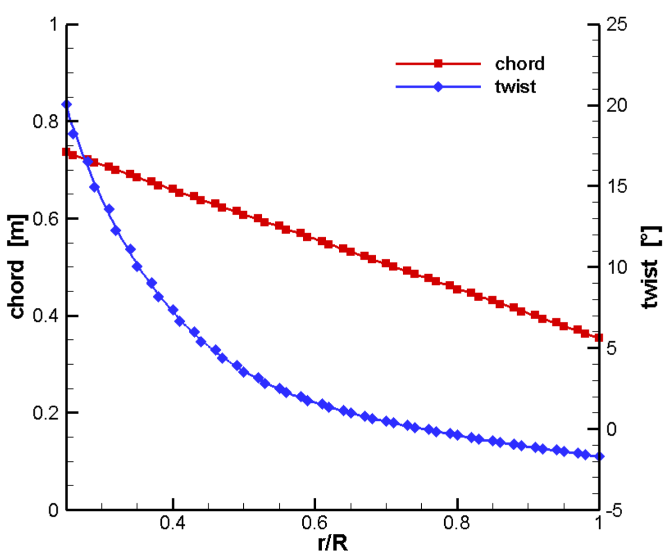

Fig. 2 – Twist and chord distribution of a twisted and tapered blade.

CFD settings

In a CFD optimization, the phase following geometry creation is the numerical evaluation, subdivided in grid creation and fluid dynamic simulation. CFD runs are the ‘high cost evaluation’ of the optimization, so that it is really vital to keep low the computational power required to perform a single evaluation. As described in the Introduction however, the CFD simulation of a wind turbine blade is a very demanding task, and the techniques adopted by the aforementioned works available in the literature are not likely to be suitable for this purpose. In a past work [19] the authors tried to speed up the overall computational simulation of a wind turbine blade while ensuring good results trustworthiness, precisely in optimization perspective. The findings of that paper are consequently employed in the present study: the main settings are reported here for clarity, whereas a detailed discussion and validation of them can be referred to the aforementioned paper [19].

Special effort has been dedicated to the computational mesh: since the overall process must be managed by computer routines and so user-independent, meshing procedure has to be completely automated. Fully unstructured grid topology with tetrahedral cells has been chosen both for surface and volumes discretization, without boundary layer refinement. Periodic conditions have been imposed in order to simulate only one blade in a moving reference frame (no nacelle and pylon interaction). The single block grid is obtained defining the point spacing on the blade surface; a size function guides the volumetric mesh, starting from blade surface itself (see Fig. 3).

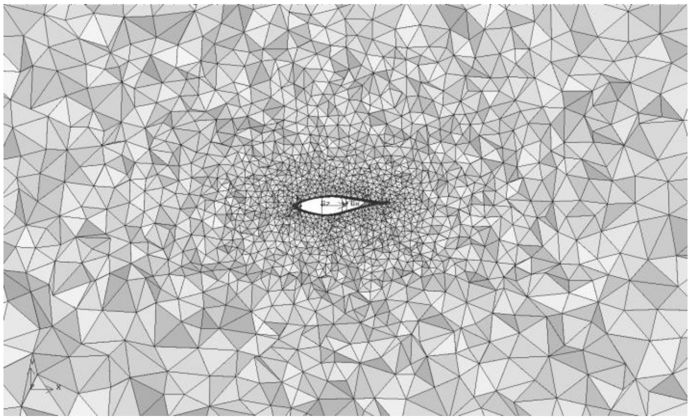

Fig. 3 – Unstructured mesh topology visualization.

Flow has been considered as steady and incompressible (assumptions fully justified by the works of Potsdam et al. [16] and Stone et al. [18]) in a constant velocity rotating reference frame, and with axial (non-yawed) conditions. Reynolds Averaged Navier Stokes approach has been used, whilst turbulence is treated with the Spallart-Allmaras model. The tools employed are the Ansys Fluent® package with its pre-processor Gambit®, both executed in batch mode by journal file routines.

Combining all the aforementioned simplifications, a 3D CFD computation of a small wind turbine blade requires only less than 3 hours on a common desktop PC, which is an affordable cost for a CFD optimization process.

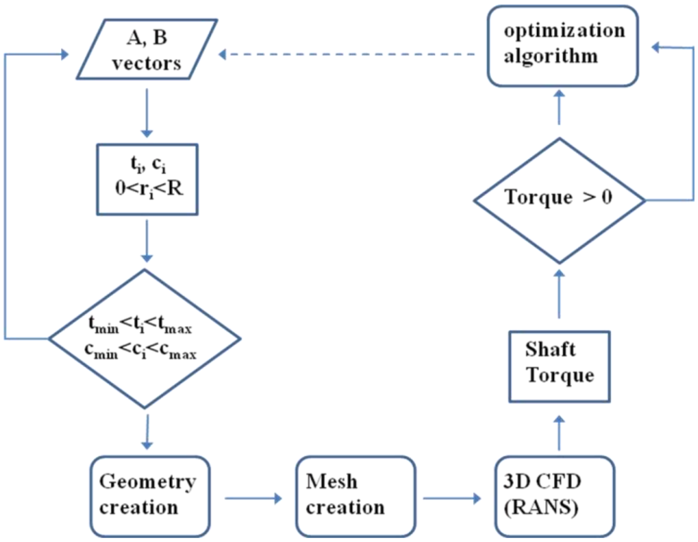

Fig. 4 – Flow chart of the optimization process.

Optimization

The last brick in the optimization process is represented by the optimization algorithm itself: once the geometry has been generated and its adherence to the objective (or objectives) has been evaluated by means of CFD, the optimization algorithm has the task of generating the new set of variables to repeat the process until convergence, as sketched in the flow chart in Fig. 4. As introduced in Fig. 4, a geometry check has been introduced in the optimization process: for each section in fact the procedure verifies that the local twist and chord are contained between a minimum and a maximum value (for example to avoid negative chords). In the present work, shaft torque is the quantity to maximize both at a single wind speed (single objective optimization, 7 m/s) and at two different wind speeds (multi objective optimization, 7 and 20 m/s). The two wind velocities are representative of attached and stalled flow conditions, again in the perspective of assessing the capability of a CFD optimization in the two cases. Each objective is reinforced by means of a constraint of positivity to enhance optimization convergence, that is, the torque in each wind condition must not be negative (otherwise the blade is not a turbine but an aerodynamic brake). Furthermore, it is convenient to point out that to optimize the shaft torque completely means to optimize the shaft power produced by the wind turbine, since the rotational velocity is constant (stall regulated wind turbine).

The tool employed to manage the overall optimization process is the software modeFrontier® by Enginsoft, which allows the use of several optimization algorithms. Given the different nature of multi- objective optimization in comparison to single- objective optimization, proper algorithms have been chosen for each optimization, i.e. the SIMPLEX algorithm has been applied to the single objective case, whilst Adaptive Range Multi Objective Genetic Algorithm (ARMOGA) have been selected for the two objectives case.

SIMPLEX algorithm is the modeFrontier® version of the well-known algorithm by Nelder and Mead [22] for non-linear single-objective optimization problems, not to be confused with the simplex method for linear programming. The SIMPLEX is not based on function derivation but on the reflection, expansion and contraction of a polyhedron containing N+1 points in a N dimensional space (where N is the number of variables), until the optimum is reached, and it is a very robust algorithm. Compared with the original, the modeFrontier® version allows also constraint violation penalty to feasibility enforcement as well as discrete variables.

The ARMOGA algorithm was originally developed by Sasaki and Obayashi [23]. With respect to traditional genetic algorithms employing selection, crossover and mutation operators to reproduce the natural evolution of species, ARMOGA also uses range adaptation to adjust the search region according to the statistics of the former data stored in an archive, see Fig. 5. Range adaption then helps reducing the number of time consuming evaluations, particularly in aerodynamic optimizations, where ARMOGA can improve multiple conflicting objectives with a low number of high cost computations.

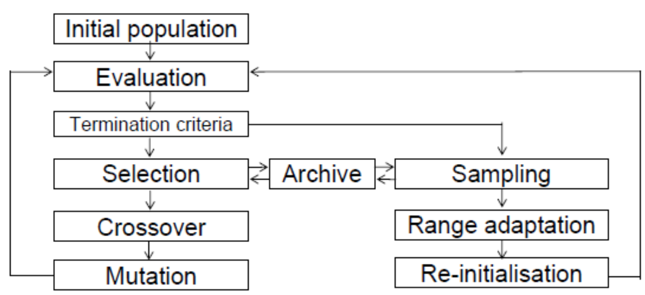

Fig. 5 – ARMOGA optimization algorithm, from [22].

RESULTS

Single-objective optimization

The single-objective (S.O.) constrained optimization has required relatively few iterations to produce a valid optimum solution. The algorithm has been initialized with a preliminary Design of Experiments (D.O.E.), made of 11 “blind” guesses pseudo-randomly generated by a SOBOL sequence. As clearly shown in Fig. 6, among D.O.E. designs only one satisfies the constraint (indicated as a red dashed line), extracting torque from the wind. Nevertheless, only 30 more designs have been necessary to converge towards positive solutions of the shaft torque. In order to assess the capability of the optimization, the results have been compared with a benchmark case, which is again the NREL Phase VI turbine blade [20]. Although the main aim of the present work is not specifically to optimize the NREL turbine, the comparison is appropriate since it has the same rotor diameter, sections profile and power regulation system (stall). The S.O. optimization final design has been compared with NREL turbine in Figures 7, 8 and 9.

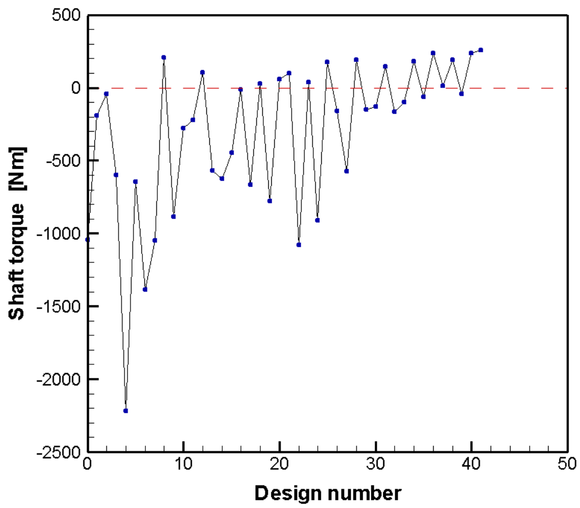

Fig. 6 – Single objective optimization history.

The first figure highlights that the optimum design has a longer chord than the NREL blade in all sections, especially at the tip. The obtained optimum is then a bigger but also heavier blade, and this could lead to structural problems; however, this matter is outside the purpose of this work, which is focused only on the aerodynamic optimization. Unlike chord, the obtained twist distribution does not show the same trend of the NREL blade; in fact, the twist angle of the blade is larger at the root, decreases steeper than the benchmark - reaching negative values at 60% span - and increases up to about + 2 degree at the tip. The optimum geometry is reported in Fig. 9 (left) together with the static pressure distribution on the pressure surface of the blade: in comparison with the NREL blade (right), pressure is slightly higher at the tip, as underlined by the colors. The combination of the aforementioned factors (chord, twist and pressure distributions) can explain the larger shaft torque produced by the final design of the S.O. optimization, which is 1.3% greater than the NREL blade. Although this small increase may be considered unnoticeable, it should be recalled that:

- wide improvements against the benchmark were not expected anyway for attached flow condition (low wind speed), because BEM design of the NREL blade is particularly robust in this condition;
- the S.O. objective has not been performed in a NREL turbine optimization perspective. The benchmark has been just used as an element of comparison, and initializing the optimization with the NREL blade instead of pseudo-random designs would have probably lead to more significant ameliorations of it;
- the object of the investigation is the possibility of successfully performing a S.O. CFD optimization of a wind turbine with given dimension and starting ideally from scratch. The obtained results confirm this possibility;
- the S:O. optimization has been regarded as an intermediate step in the direction of a more realistic multi-objective optimization. Further efforts have been dedicated then to the latter rather than continuing to develop the former.

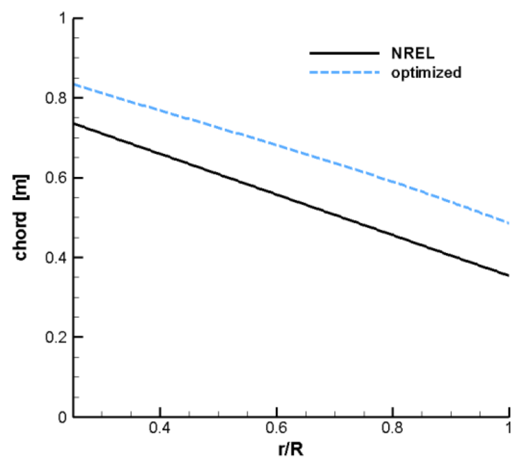

Fig. 7 – Chord distribution comparison between the best design and the NREL Phase VI blade.

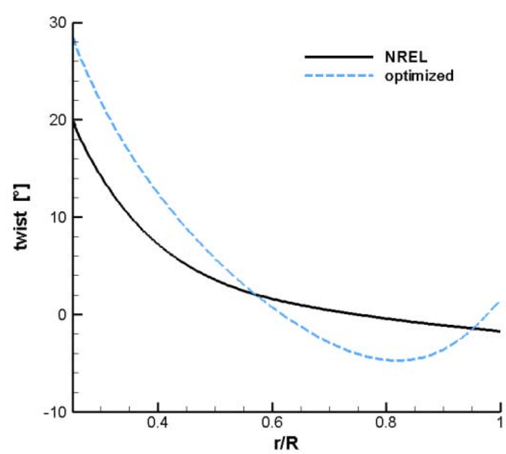

Fig. 8 – Twist distribution comparison between the best design and the NREL Phase VI blade.

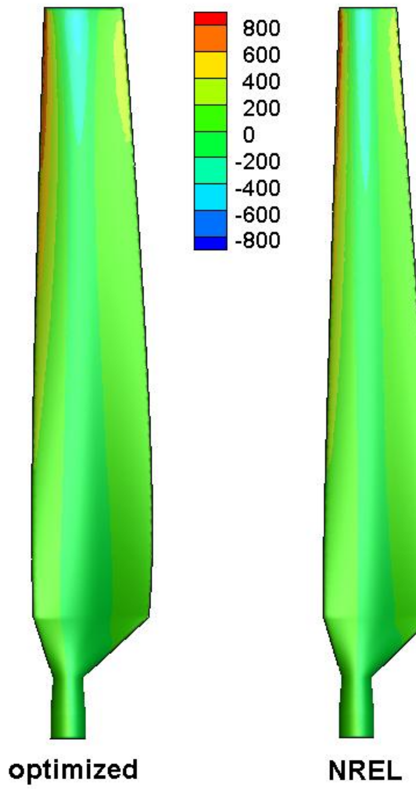

Fig. 9 – Static pressure distribution comparison between the S.O. optimum and the NREL Phase VI blade (front view).

<u>Multi-objective optimization</u>

In a multi objective (M.O.) constrained optimization, the algorithm performs a trade-off between different objectives, so that the optimization history of a single objective is not much revealing. The selection of the optimum is usually made between the individuals lying on the Pareto Front, that is the set on non-dominated solutions. In Fig. 10, the two-dimensions objective space of the proposed M.O. optimization is represented: the individuals generated by the ARMOGA algorithm are spread over the whole plot, but the two red dashed lines define the feasible region in the right-up sector where both constraints are satisfied (a SOBOL D.O.E. has been used also in this case). The Pareto Front is shown with a green line and joins together the feasible designs able to maximize one objective for a given value of the other objective. Once the Pareto Front has been individuated, the selection of the optimum individual is completely up to the importance given to one objective in relation to the other. In the present study, the best design has been chosen in order to maximize the low speed torque first, and so the optimum is the individual with the highest torque at the lowest wind velocity (circled in red in Fig. 10). This decision can be justified considering that the wind turbine is supposed to spend a larger part of its operational time working at this wind speed condition: consequently, it is more convenient to improve this condition first (it can be also noticed from the plot that the other designs with bigger high speed torque are characterized also by an unacceptable shaft torque at low wind velocity).

As previously done in S.O. optimization, also in this case the selected optimum has been compared with the NREL benchmark, again by means of chord (Fig. 11), twist (Fig. 12) and pressure distributions (Fig. 13).

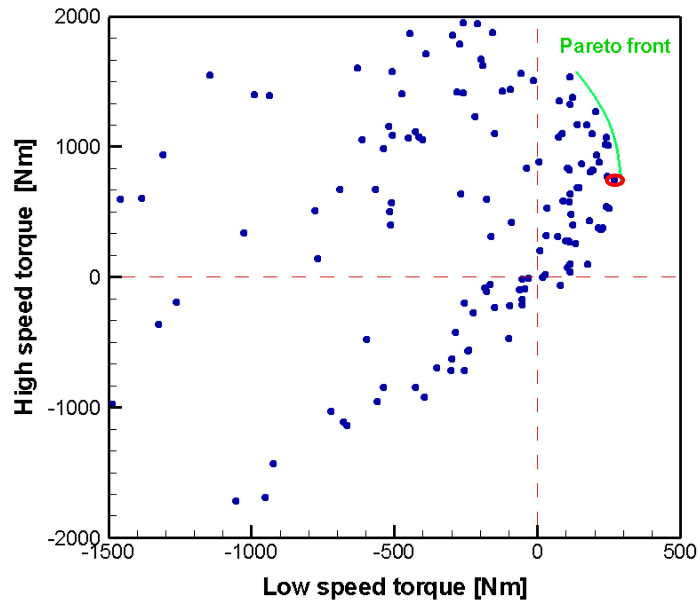

Fig. 10 – Multi objective optimization Pareto front.

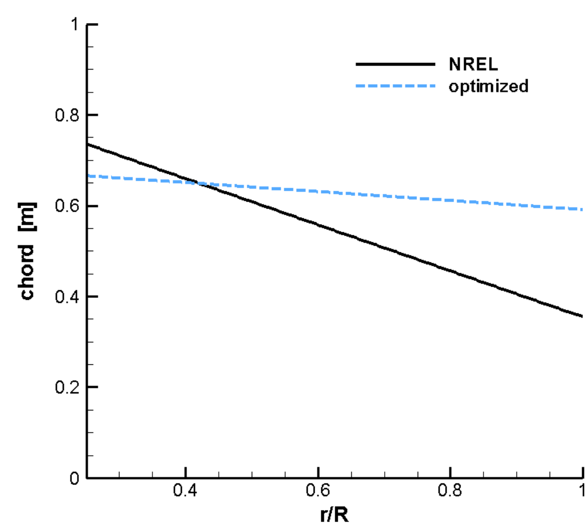

Fig. 11 – Chord distribution comparison between the M.O. optimum and the NREL Phase VI blade.

The M.O. optimum shows an interesting chord distribution: it is lower than NREL blade at the root but greater than the benchmark elsewhere, with an intersection at about 40% of the blade span. Twist distribution is quite similar to the one obtained with the S.O. optimization, since it has the same trend; however, values are slightly different: at the blade root the angle is bigger, whereas the excursion in the negative region is less pronounced.

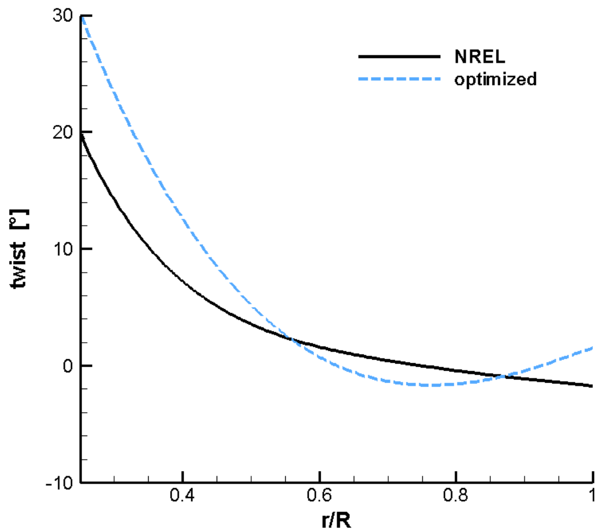

Fig. 12 – Twist distribution comparison between the M.O. optimum and the NREL Phase VI blade.

Figure 13 reveals a pressure distribution of the best individual very close to the NREL blade: both shape and values of the contours are very similar, apart from the nearly constant chord of the optimized blade. Nevertheless, the increased chord together with changed angles of attack lead to marked torque increase: above 35% in the high speed condition and 7% in the low speed condition on the benchmark. As expected, stalled conditions are more likely to be optimized than attached flow conditions, because CFD becomes more valuable in the former case. It is also of interest to stress that those improvements in blade design have been obtained without even changing the blade profile: future works will concentrate on this issue, and further ameliorations are expected. In addition to aerodynamics, optimizations to come should also include structural integrity as an objective, due to its relevance for wind turbines. This could be done for example joining Finite Element Method (F.E.M.) and CFD in a multi-disciplinary and multi-objective environment, also considering more than two wind velocities.

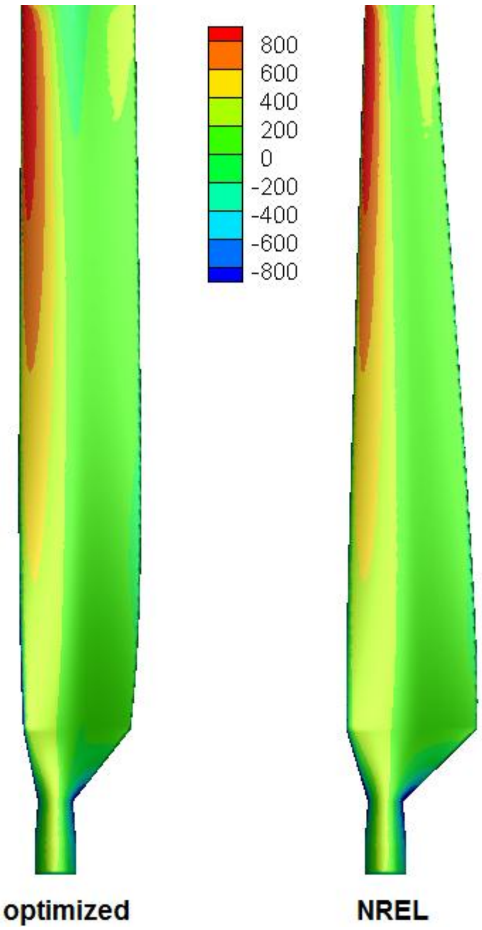

Fig. 13 – Static pressure distribution comparison between the M.O. optimum and the NREL Phase VI blade (front view) at high speed condition.

CONCLUSIONS

In the present work, the possibility of using CFD instead of BEM in a wind turbine optimization is explored. Starting from the simplifications previously introduced by the authors in wind turbine CFD simulations, a single and multi objective aerodynamic optimization has been performed, including feasibility constraints.

The obtained results indicate that a CFD optimization is affordable when applied to stall regulated wind turbines, and can lead to optimum designs starting just from a pseudo-random initialization of the parameters. A comparison with the well known NREL Phase VI turbine shows significant improvements can be achieved even keeping fixed the aerodynamic profile and varying only twist and chord distributions of the blade, particularly for stalled conditions. Optimum designs are characterized by larger chords, especially at the blade tip; then, it may be appropriate in the future to include also structural analyses in the optimization.

NOMENCLATURE

a	twist distribution polynomial coeff.	
A	vector of twist coefficients	
b	chord distribution polynomial coeff.	
B	vector of chord coefficients	
c_i	chord of the i-th section	[m]
C_d	drag coefficient	
C_l	lift coefficient	
C_N	normal force coefficient	
C_T	tangential force coefficient	
r_i	radial coordinate of the i-th section	[m]
R	blade span	[m]
t_i	twist of the i-th section	[°]

Greek

Φ	angle of twist	[°]

REFERENCES

[1] European Wind Energy Association (2010), "EWEA Annual Report 2009", available at www.ewea.org.

[2] Global Wind Energy Council (2010), "Global Wind 2009 Report", available at www.gwec.net.

[3] Giannakoglou, K.C. (1999), "Designing turbomachinery blades using evolutionary methods", in Proceedings of ASME Turbo Expo 1999, Indianapolis, USA, June 1999, ASME Paper 99-GT-181.

[4] Verstraete, T., Alsahili, Z., and Van den Braembussche, R. A. (2010), "Multi-disciplinary Optimization of a Radial Compressor for Micro Gas Turbine Applications", *ASME Journal of Turbomachinery*, **132**, 3, July 2010.

[5] Verstraete, T., Garreau, M., Alsahili, Z., and Van den Braembussche, R. A. (2007), ""Multi-disciplinary Optimization of a Radial Turbine for Micro Gas Turbine Applications", in Proceedings of the 7th European Conference on Turbomachinery, pp. 667-676, Athens, Greece, 2007.

[6] Milli, A., Shaphar, S. (2008), "Full-Parametric Design system to improve the stage efficiency of a High-Fidelity HP Turbine configuration", in Proceedings of ASME Turbo Expo 2008, Berlin Germany, 2008, GT2008-51348.

[7] Albadi, M.H., El-Saadany, E.F. (2010), "Optimum turbine-site matching", *Energy*, **35**, pp. 3593-3602.

[8] Kongnam, C., Nuchprayoon, S.(2010), "A particle swarm optimization for wind energy control problem", *Renewable Energy*, **35**, pp. 2431-2438.

[9] Fuglsang, P., Madsen, H.A. (1999), "Optimization method for wind turbine rotors", *Journal of Wind Engineering and Industrial Aerodynamics*, **80**, pp. 191-206.

[10] Lanzafame, R., Messina, M. (2007), "Fluid dynamics wind turbine design: Critical analysis, optimization and application of BEM theory", *Renewable Energy*, **32**, pp. 2291–2305.

[11] Hao Xuan, Zhang Weimin, Liu Xiao and Liu Jieping (2008), "Aerodynamic and Aeroacoustic Optimization of Wind Turbine Blade by a Genetic Algorithm", in Proceedings of 46th AIAA Aerospace Sciences Meeting and Exhibit, January 2008, Reno, Nevada, AIAA 2008-1331.

[12] Wang Xudong, Wen Zhong Shen, Wei Jun Zhu and Sørensen, J.K., Chen Jin (2009), "Shape Optimization of Wind Turbine Blades", *Wind Energy*, **12**, pp. 781–803.

[13] Hansen, M.O.L. (2008), "Aerodynamics of Wind Turbines", Earthscan publications, London, UK.

[14] Sørensen, N.N., Michelsen, J.A., Schreck, S. (2002), "Navier-Stokes predictions of the NREL phase VI rotor in the NASA Ames 80-by-120 wind tunnel", in Proceedings of ASME 2002 Wind Energy Symposium (WIND2002) January 2002 , Reno, Nevada.

[15] Duque, E.P.N., Burklund, M.D., Johnson, W. (2003), "Navier-Stokes and comprehensive analysis performance predictions of the NREL phase VI experiment", *Journal of Solar Engineering*, **125**, pp. 457–467.

[16] Potsdam, M. A., Mavriplis, D. J. (2009), "Unstructured Mesh CFD Aerodynamic Analysis of the NREL Phase VI Rotor", in Proceedings of 47th AIAA Aerospace Sciences Meeting and Exhibit Proceedings, January 2009, Orlando, Florida, AIAA 2009-1221.

[17] Gomez-Iradi, S., Steijl, R., Barakos, G. N. (2009), "Development and Validation of a CFD Technique for the Aerodynamic Analysis of HAWT", *Journal of Solar Engineering*, **131**, 3, August 2009.

[18] Stone, C., Lynch, C. E., Smith, M. J., 2010. "Hybrid RANS/LES Simulations of a Horizontal Axis Wind Turbine". In 48th AIAA Aerospace Sciences Meeting Including the New Horizons Forum and Aerospace Exposition Proceedings, Orlando, Florida, AIAA 2010-459.

[19] De Bellis, F.; Catalano, L.A., Dadone, A., "Fast CFD simulation of horizontal axis wind turbine", in Proceedings of ASME Turbo Expo 2009, June 2009, Glasgow, UK, GT2010-22724.

[20] Simms, D., Schreck, S., Hand, M., Fingersh, L.J. (2001),. "NREL unsteady aerodynamics experiment in the NASA Ames wind tunnel: a comparison of predictions to measurements, NREL/TP-500-29494".

[21] Tangler, J., Somers, D. (1994), "Status of the NREL airfoil design efforts", American Society of Mechanical Engineers, Solar Energy Division (Publication) SED, 15, p. 7.

[22] Nelder, J. A., Mead, R., (1965), "A simplex method for function minimization", *Computer Journal*, **7**, pp. 308-313.
[23] Sasaki, D., Obayashi, S. (2005), "Efficient Search for Trade-Offs by Adaptive Range Multi-Objective Genetic Algorithms," *Journal of Aerospace Computing, Information, and Communication*, **2**, pp. 44-64.